Journal of Fluorescence, Vol. 11, No. 1, 2001

Spectral Properties of Bacteriochlorophyll *c* in Organisms and in Model Systems

Jacek Goc,[1] Alina Dudkowiak,[1] Zygmunt Gryczyński,[2] Ignacy Gryczyński,[2] Bogumil Zelent,[2] and Danuta Frąckowiak[1,3]

Received July 28, 2000; revised December 18, 2000; accepted December 22, 2000

Polarized absorption and fluorescence spectra of bacteriochlorophyll *c* and green photosynthetic bacterium *Prostheecochloris aestuarii* cells and cell fragments embedded in stretched polymer film were measured. In pigment samples the artificial oligomers of bacteriochlorophyll *c* (with absorption about 750 nm) and other forms of this pigment and bacteriopheophytin (with absorption at 670 nm) were present. In bacteria samples, embedded in polymer, oligomers were in high degree disaggregated and as a result the absorption about 670 nm was observed. Previously for similar sets of samples the decay of fluorescence excited only at one wavelength was analyzed on three exponential components, but exact lifetime values of these components for various samples were different. The aim of present paper was to check if these differences occur because of various contributions to decay from three well defined forms or if they were related to the existence of several pigment forms with slightly different lifetimes. The global analysis of data obtained for various excitation and observation wavelengths of fluorescence were done. From this analysis it follows that the second situation occurs. For a model system containing artificial oligomers the largest component of decay has a τ^4 of about 0.183 ns or 0.136 ns depending on observation wavelength. For the bacteria sample, in which the emission at 680 nm is the superposition from various pigments, global analysis done for various excitation wavelengths shows also that the τ values differ depending on the regions of fluorescence observation. From polarized spectra, it follows that in the model system the pigments absorbing at 670 nm are randomly distributed whereas oligomers are highly oriented. In bacteria fragments absorbing at 670 nm pigment molecules can be divided into two groups: one oriented along the axis of film stretching and the second practically randomly distributed. In living organisms, under some conditions, small amount of 670 nm pigments can be present and can work as excitation energy traps or as antenna transferring the excitation. Present results show that the role of various pools of 670 nm absorbing pigments can be different because of their differing orientation.

KEY WORDS: Bacteriochlorophyll *c*; green bacteria; lifetime of fluorescence; oligomers of bacteriochlorophyll *c*; polarized spectroscopy; polymer films.

INTRODUCTION

It is known, that from polarized absorption and fluorescence spectra of oriented dyes it is possible to draw information about the location of absorption and fluorescence transition moments (TMs)[4] in a frame of molecule as well as about the influence of local electric fields and interactions with surroundings on pigment spectral

[1] Institute of Physics, Poznań University of Technology, Nieszawska 13, 60 965 Poznań, Poland.

[2] Center for Fluorescence Spectroscopy, University of Maryland, School of Medicine, Department of Biochemistry and Molecular Biology, 725 West Lombart Street, Baltimore, Maryland 21201.

[3] To whom correspondence should be addressed. Fax: +48 +61 6652324. E-mail: frackow@phys.put.poznan.pl

[4] *Abbreviations used:* absorption anisotropy (s): bacteriochlorophyll (BChl): bacteriopheophytin (BPhe); dichroic ratio (R_2); lifetime (τ); polyvinyl alcohol (PVA); Fenna–Mathews–Olson complexes (FMO); transition moments (TMs).

1053-0509/01/0300-0053$19.50/0

properties [1–3]. Different set of information can be obtained from oriented small organisms cells or cell fragments. Predominantly such information concerns the location of chromophores inside organisms but also exhibits the influence of the surroundings on pigment properties [4,5]. Orientation can be reached by the location of dye or larger objects in anisotropic films [1,6–11], in nematic liquid crystals [12–14] or other anisotropic systems [2,15,16–20]. From fluorescence lifetime measurements one can gather information about the fate of excitation energy in investigated system. For photosynthetic antenna complexes very important is the deactivation of excited pigment molecule by the excitation energy transfer to other antenna or to reaction center.

The green sulfur bacterium *Prosthecochloris aestuarii* contains light-harvesting complexes called chlorosomes. The main pigment of chlorosome is bacteriochlorophyll (BChl) *c* with a small admixture of BChl *a*. From the comparison of theoretical predictions with experiments such as spectral hole burning [17], fluorescence spectra [18] or other spectral results [19,20] it follows that BChl *c* molecules are arranged in chains located on the surface of the rod elements and built from pigment molecules strongly interacting between themselves [19,20]. The properties of exciton generated by illumination of chlorosome pigments were established [17,21,22]. Previously [9] we have established, on the basis of bacteria photographs done under fluorescence microscope combined with polarized absorption and fluorescence spectra, that Q_y transitions of chlorosomal BChl *c* are almost parallel to the long axis of chlorosomes. This result is in agreement with chlorosome models proposed in literature [17,18,19,20]. We had measured also the fluorescence lifetimes of oriented bacteria, their fragments and artificial BChl *c* oligomers [7]. Because of technical difficulties the lifetimes were measured previously [7] only at one wavelength of exciting light. The decay of emission was analyzed using three components. The lifetimes and the amplitudes of these components were not dramatically changed with the change in polarization of exciting and emitting light [7].

The lifetime (τ) in the present paper was measured for several wavelengths of exciting and fluorescence light using the method of frequency domains [23] whereas previously [7] the method of time domains was applied. Now only unstretched isotropic samples under magic angle conditions were investigated. Stretching deforms large objects such as bacteria and as a result changes mutual orientation of various TMs [9,24]. The lifetime values for stretched samples were similar for different light polarizations [7], therefore we now decided to use unpolarized light for fluorescence excitation in lifetime experiments. The aim of this paper is to follow the role of the various pigment forms in excitation energy transfer and fluorescence emission, we therefore apply three excitation wavelengths characteristic of three main forms (BChl *c* monomers, bacteriopheophytin (BPhe) *c* and BChl *c* oligomers) and two regions of observations 680 nm characteristic of monomers and small aggregates and 750 nm characteristic of oligomers. Global analysis was applied to the set of results obtained for various excitations. In the case where only three supposed groups of chromophors exist in a sample the analysis for both regions of fluorescence observation should give the same sets of lifetimes values.

From the investigation of bacteria [7,9,24] and model systems containing BChl *c* aggregates [12,24–27] it is known that there exist in organisms and in model systems not only monomers of pigment and large oligomers but also several other forms (small aggregates—probably tetramers, BPhe *c*, etc). The supposition that BChl *c* fluorescence lifetime can be analyzed on only three components may be an oversimplification. In this paper we again very carefully measured and analyzed polarized absorption and fluorescence of bacteria, bacteria fragments for artificial oligomers in order to gather information about orientation of pigments TMs For the same, but isotropic samples, the fluorescence lifetimes were measured at various wavelengths of excitation and observation and the global analysis of lifetimes was done. On the basis of previous results [9,12,24,25] the wavelengths of excitation and observation were chosen in the regions of the strong absorption and emission of various BChl *c* forms.

MATERIALS AND METHODS

Materials

The culture of green sulfur bacterium *Prosthecochloris aestuarii* 2K strain, isolation of mixture of homologs BChl *c* by thin–layer chromatography [28], introduction of the sample into polymer film, and film stretching procedure were described previously [9]. By the resin addition the pH 7.0 of polyvinyl alcohol (PVA) sample was reached. PVA films were stretched uniaxially up to 200% of their initial length. Bacteria fragments were obtained by sonication for 15 min. at 4 °C and centrifugation at 36 000 × g. According to our previous results [29] the chlorosomes are present in our green bacteria culture. After introducing the bacteria into PVA film, as it follows from the growing ratio of absorbtion maxima at 674 nm to that at 752 nm, chlorosomes undergo

partial disaggregation. Already previously [7,9,24] was reported that the sonication of bacteria as well as the storage of whole bacteria in PVA film causes disaggregation of BChl *c* oligomers in chlorosomes, but monomers and smaller aggregates are still to some extend oriented. Artificial oligomers of BChl *c* in PVA are very stable. For lifetime measurements only unstretched films were used.

Absorption and Fluorescence Spectra

Polarized absorption components were measured by placing a Glan Polarizer in front of the sample inside a AVIV 14DS spectrophotometer. The absorption of the sample was corrected for a baseline obtained with blank PVA film, then corrected for the film absorption calibrated for the thickness. The dichroic ratio (R_d), it means the ratio of absorption of light polarized parallel to the direction of stretching (A_{II}) to that polarized perpendicular to this direction ($A_{\perp}$) is shown in the figures. It is related to absorption anisotropy (*s*) by the following formula:

$$R_d = \frac{A_{II}}{A_{\perp}} = \frac{2s + 1}{1 - s} \quad (1)$$

$$s = \frac{A_{II} - A_{\perp}}{A_{II} + 2A_{\perp}} \quad (2)$$

Values of *s* for various regions of absorption were also calculated. This permits the comparison of current presented and previous [9,25] data.

Fluorescence spectra measurements for different PVA films were performed in SLM 8000 fluorometer using spatially designed front face adapter as shown in Fig. 1a. To avoid any depolarization effects the film surface was placed orthogonally to the direction of observation. This configuration allows easy measurements of emission polarization as well as the measurements of the spectra under magic angle conditions [30,31].

For excitation the same wavelengths characteristic of absorption of various species were used as are given in description of lifetime method. The components of polarized emission are marked in following way: the first and last letter show the directions of electric vector of light in exciting and fluorescence beams, whereas the middle letter refers to the position of polymer film stretching axis. It is 0 for unstretched films. V (vertical) and H (horizontal) directions.

Lifetime Measurements and Analysis

The phase and modulation (frequency domain) lifetime measurements were done for unstretched films under magic angle conditions using the same front face adapter. Excitation was provided by a mode-locked Ti-sapphire laser (Tsunami from Spectra Physics) (Fig. 1b). The repetition rate of 80 MHz and power of about 1 W was divided down to 4 MHz. The Ti-sapphire laser output (780 nm–900 nm) was frequency-doubled using an Inrad model 5-050 doubler/tripler. The emission was isolated using an interference filter together with cutoff filters.

For excitation, the following wavelengths located in Soret band: 420 nm (BPhe *c* monomer absorption), 438 nm (monomers and small aggregates of BChl *c* absorption) and 450 nm (predominant BChl *c* oligomers absorption) were used.

Fluorescence for lifetime measurements was gathered in a region at 680 nm (emission of monomers and small aggregates of BChl *c* and BPhe *c*) and at 750 nm (predominantly BChl *c* oligomers fluorescence).

The absorption and fluorescence bands of various forms of pigments are strongly overlapped. The way to improve the resolution of the different lifetimes of fluorescence emitted by such biological samples is global analysis of the lifetime results [23]. Global analysis is based on the assumption that decay time of a given component is independent of fluorescence and excitation wavelengths. In our case we did some oversimplification supposing that only three emitting species are present in a sample. It is known that even oligomers occur at least in two different forms [32,33]. Also small aggregates could be not uniform. Previous [7] lifetime results obtained on a similar set of samples show that in approximation decay times can be divided into three groups: longest times are characteristic of monomers (from 5.6 ns to 7.4 ns), the intermediate time (1.1 ns–2.7 ns) are probably due to small aggregates of BChl *c* and the shortest time (0.001 ns–0.37 ns) are related to oligomers. Actually, we want to use the global analysis to check if such division into only three types of decays is reasonable. We suppose for our analysis that decay of fluorescence is a superposition of three or less exponential components. Supposition of monoexponential decay for each component is not a good approximation for mutually closely located and strongly interacting BChl *c* molecules in chlorosomes [17–20]. We had shown previously [10] that in a case of oligomer fluorescence decay is better approximated by fractal model with a stretched exponent than by monoexponential formula. But the supposition of two exponential decays and one with stretched exponent introduces many arbitrary constants. We therefore decided to try to analyze decays with three exponential components:

$$I(t) = \sum_{i=1}^{3} \alpha_i \exp\left(\frac{-t}{\tau_i}\right) \quad (3)$$

where α_i is the amplitude of *i*-component at t = 0 and

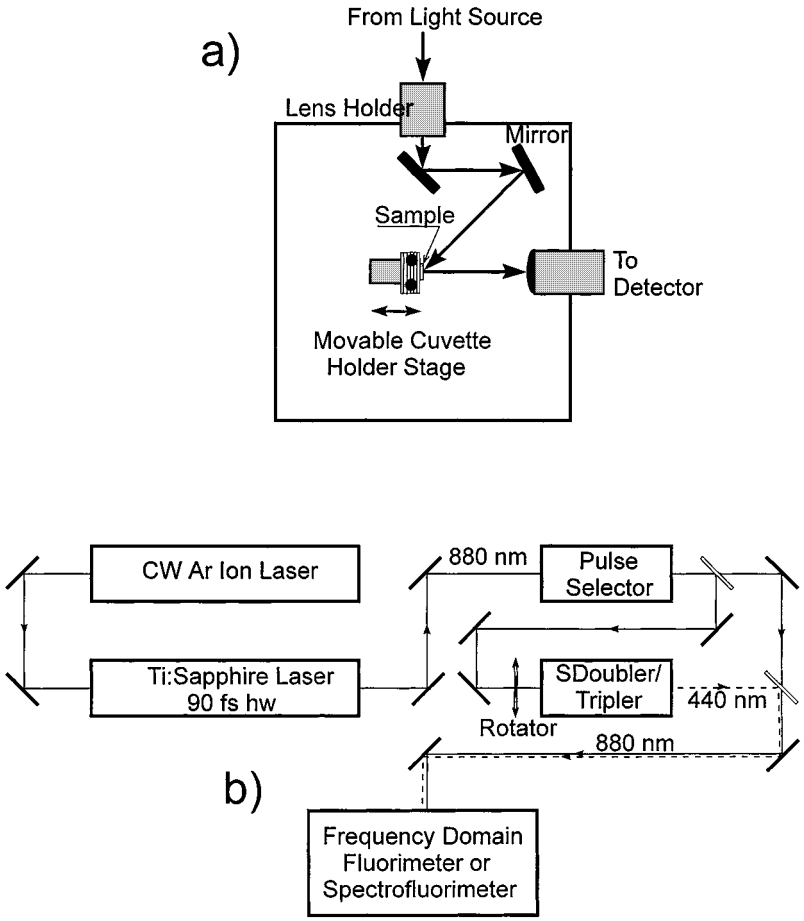

Fig. 1. Scheme of fluorescence front face sample holder (a) and excitation source (b).

τ_i is the decay time of *i*-component. In some cases the acceptable fit is reached with a lover numbers of *i*-components.

The fractional contribution (f_i) of each decay time to the steady state intensity is

$$f_i = \frac{\alpha_i \tau_i}{\sum_{j=1}^{3} \alpha_j \tau_j} \tag{4}$$

where $\alpha_i \tau_i$ is proportional to the area under the decay time for *i*-component (it is weaker for shorter times). The result of the average lifetime $\langle \tau \rangle$ is also given:

$$\langle \tau \rangle = \sum_{i=1}^{3} f_i \tau_i \tag{5}$$

Experimental data in the frequency domain lifetime measurements are usually [23] presented as increasing values of the frequency dependent phase angle ($\Phi_{\bar{\omega}}$) and decreasing values of the modulation ($m_{\bar{\omega}}$). Examples of such curves obtained for whole bacteria sample for various excitations and 750 nm observation are presented in Fig. 2. As can be seen from this example the fitting was very good.

RESULTS AND DISCUSSION

Model System: BChl *c* in PVA

Figure 3 shows the polarized absorption spectra of BChl *c* in PVA. The parallel and perpendicular components of absorption were normalized. In the same figure the dichroic ratio is shown. The sample contains a high concentration of oligomers (maximum at about 750 nm), and monomers (with absorption at about 670 nm). As it follows from dichroic ratio (R_d =2.15 at 744 nm and 2.07 at 744 nm, accuracy $\pm$0.02) oligomers show a high degree of orientation parallel to the PVA axis of film

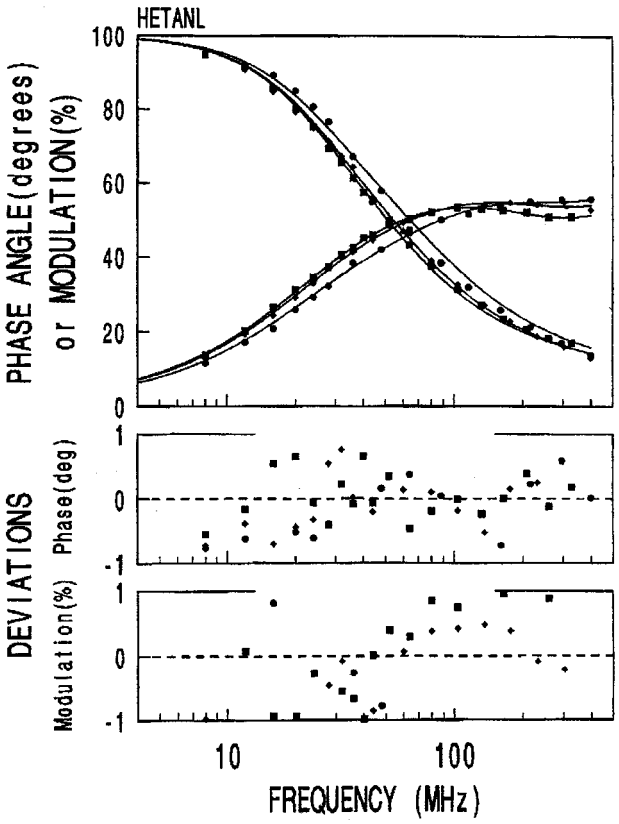

Fig. 2. Frequency response of BChl *c* fluorescence intensity decays in PVA film observed at λ_{em} = 750 mm. The solid lines represent the best global analysis of three-exponential fit to the data at λ_{exc} = 450 nm (circles), λ_{exc} = 438 nm (small squares) and λ_{exc} = 420 nm (squares).

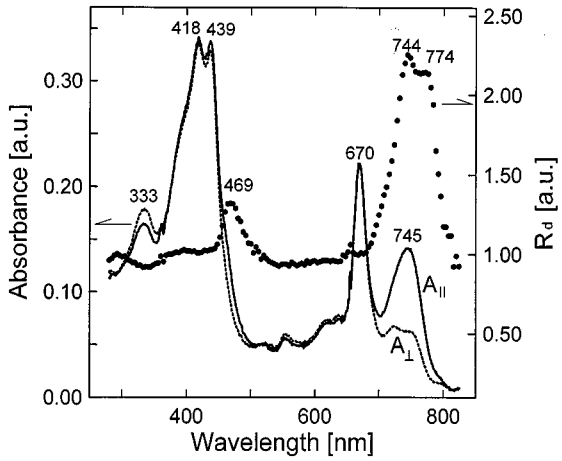

Fig. 3. Normalized parallel (A_{II}, solid line) and perpendicular ($A_{\perp}$, dashed line) components of absorption spectra and dichroic ratio R_d = $A_{II}/A_{\perp}$ (dotted line) of BChl *c* in PVA.

stretching. From the shape of $A_{\perp}$, as well as from R_d values it follows that at least two types of oligomers are present (with maxima at 744 nm and 774 nm). This is in agreement with data from the literature [32] describing two BChl *c* forms in natural chlorosomes with absorption maximum at 753 nm and 769 nm. In [9] two types of clusters (735 and 769 nm) were also suggested. Anisotropy of absorption in a Soret band for all chlorophylls is much lower than that in a red band [8,34]. Now R_d at 469 nm is only 1.27. This is due to strong overlapping of B_x and B_y TMs in Soret band. The small maximum of R_d at about 469 nm can be due to anisotropy of oligomeric forms. Very characteristic of the investigated sample is the practically random orientation of monomeric forms of pigments ($R_d \cong 1{,}03$ at 670 nm). Previously [12,13,34] in nematic liquid crystals monomeric pigment molecules were well oriented. Most chlorophylls in stretched PVA exhibit high degree of orientation [8]. Low orientation of BChl *c* monomers can be due to a rather low degree of film stretching (200%) and resin addition. Any way from the results shown in Fig. 3 and a strong difference between the orientation of monomers and oligomers is easily seen. The *s* values (now for monomers about 0.01 and for oligomers from 0.26 to 0.28) were lower than those ($s \approx 0.85$ for monomers and about 0.74 for oligomers) observed previously in a liquid crystal matrix [26].

Figures 4a–c show the polarized fluorescence spectra (shape of *VVV* and *VVH* normalized components and their intensities ratio) of the same sample at various wave-

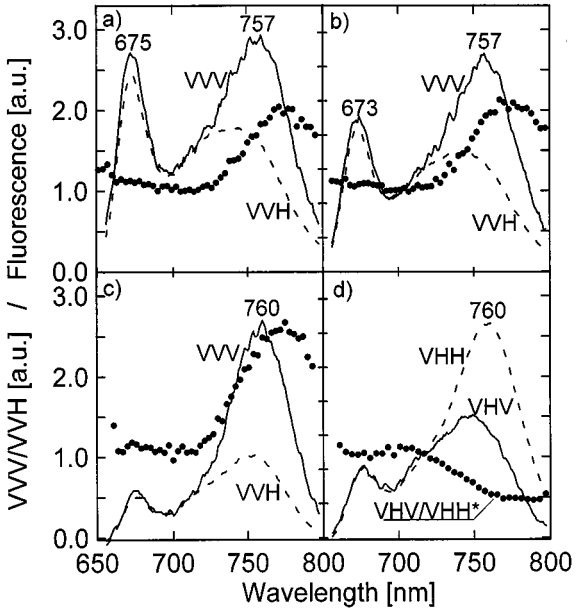

Fig. 4. Polarized fluorescence components and their intensities ratios (*VVV*/*VVH* or **VHV*/*VHH*, shown as dotted line) or BChl *c* in stretched PVA: (a) *VVV*/*VVH*, λ_{exc} = 420 nm, (b) *VVV*/*VVH*, λ_{exc} = 438 nm, (c) *VVV*/*VVH*, λ_{exc} = 450 nm, (d) *VHV*/*VHH*, λ_{exc} = 450 nm. Explanation of components notation is given in text.

lengths of excitation. In all cases *VVV*/*VVH* is about one in the region of monomeric emission (660 nm–700 nm), whereas in the oligomeric region (760 nm–780 nm) it is about two and at 450 nm excitation as high as 2.6. This is in agreement with R_d absorption data showing high orientation of oligomers. Because of the superposition of emissions from various forms the shapes of fluorescence components at various excitations are different. In random orientation the change of film axis has no influence on fluorescence polarization and VVV/VVH as well as *VHV*/*VHH* have to be similar. This ratio is about one in monomer region. The values of:

$$r_a = \frac{VVV - VVH}{VVV + 2VVH} \tag{6}$$

were also calculated. In monomer region (660 nm–700 nm) at all excitation wavelengths (420 nm, 438 nm and 450 nm) r_a is from 0.02 to 0.03, whereas in oligomers region (760 nm–780 nm) from 0.23 to 0.27. These values are lower than observed previously [12,26] in liquid crystal matrix (r_a was about 0.5 for monomers and 0.5–0.9 for oligomers).

Figure 4d shows polarization of emission of molecules located with their TMs at a large angle with respect to the film axis (*VHV* and *VHH* components) measured at 450 nm excitation. In the monomer region *VHV*/*VHH* is still equal about one, but in the oligomer region it is about 0.5. It shows the existence of some oligomeric species with TMs of absorption and emission located at a large angle with respect to the PVA axis. Similar effect was observed at other wavelengths of excitation. The values of:

$$r_b = \frac{VHV - VHH}{VHV + 2VHH} \tag{7}$$

are also calculated (r_b for monomers is equal 0.02, for oligomers -0.2). The comparison of *s* values with r_a values shows that BChl *c* oligomers exhibit a higher orientation degree of absorption and emission TMs than that of monomers. It is known that the angle between TM of absorption and emission for most of chlorophylls molecules is low [3]. Negative values of r_b (about -0.02 in oligomer emission region at 450 nm excitation) show that VHH > VHV it means molecules with TMs oriented at a large angle to PVA axis possess also TMs of fluorescence forming large angle.

Whole Bacteria Cells and Cell Fragments in PVA Films

Figure 5 shows polarized absorption and the dichroic ratio of polarized components for whole bacteria cells

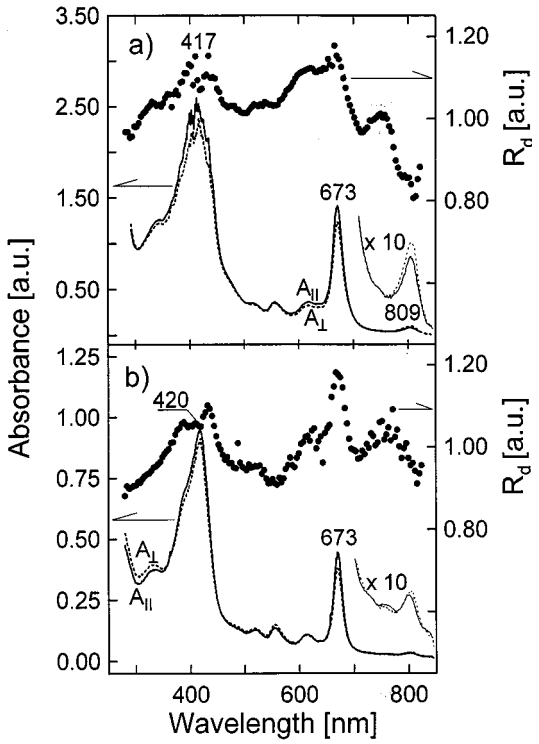

Fig. 5. Polarized absorption spectra and dichroic ratio R_d of: (a) whole cells, (b) cell fragments in stretched PVA (insert in expanded scale). Description of curves as in Fig. 3.

(Fig. 5a) and cell fragments (Fig. 5b). As was mentioned in Material and Methods, the oligomers of BChl *c* are to a great extent disaggregated (low 750 nm absorption). In bacteria the monomers are ordered, as was also observed previously [9,27]. Whole large objects (bacteria or bacteria fragments) are now oriented and as a result of inner ordering of monomeric pigment molecules anisotropy in 680 nm region is observed ($R_d \approx 1.15$). At low degree of stretching large objects can be more easily oriented than separated molecules. From the spectra in Fig. 5 the absorption of oligomers in 750 nm region is practically not seen, but the R_d maxima in 750 nm–770 nm and 450 nm suggest that a small amount of BChl *c* oligomer is still present and exhibits different orientation than that of monomer ($R_d < 1$). BChl *a* from baseplate absorbs at 793 nm–795 nm and from Fenna-Mathews-Olson (FMO) complexes at 809 nm [9,35]. Dichroism of FMO complexes has been reported recently by Melkozerov *et al.* [35] measured in squeezed gel. The dichroism obtained by these authors was similar to that presented in Fig. 5. It seems, from the insert in Fig. 5, that various pools of BChl *a* are differently oriented. A similar conclusion follows from the literature [36].

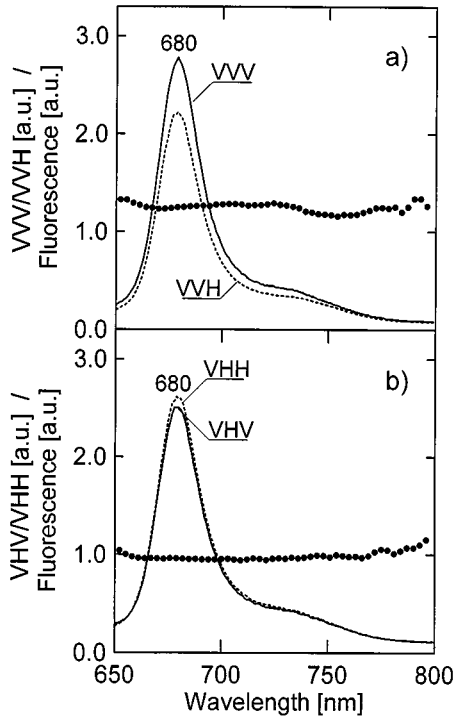

Fig. 6. Spectra of polarized fluorescence (λ_{exc} = 450 nm) and their intensities ratio (dotted lines) for whole bacteria cells: (a) for *VVV* and *VVH* components, (b) *VHV* and *VHH* components.

Figure 6 shows the polarized fluorescence spectra of bacteria. At all excitation wavelengths for whole bacteria and bacteria fragments *VVV*/*VVH* ratio changes from 1.25 to 1.41. It shows that the emitting molecules exhibit a higher degree of orientation than the average orientation of all the absorbing molecules. The *VHV*/*VHH* ratio is from 0.88 for bacteria cells (Fig. 6b) to 0.94 for bacteria fragments (not shown), showing that the other molecules, except these which are ordered along orientation axis, are almost randomly distributed. The situation is similar in bacteria and bacteria fragments, at various λ_{exc}, therefore only some examples are presented in Fig. 6.

In all our samples several pools of pigment molecules with strongly overlapping spectra and various orientations are present. Therefore it is not reasonable to introduce a stepwise procedure for obtaining the component of TMs located in the frame of molecules such as is usually applied to dye in stretched polymer films or liquid crystal cells [1,2,8,13,25,34]. From this literature we know the location of TMs of BChl *c* in the porphyrin ring. Transition moments of Q_y is almost parallel to the line connecting I and III pyrole rings. Of course, due to intermolecular interactions, the directions of TMs can be slightly changed, but in case of our complicated systems such effects are in a limit of accuracy. From polarized spectra we infer the existence of various pools of pigment "forms" and their location in the systems being under investigation.

Lifetime Measurements of BChl *c* in Model Systems

The simplest lifetime results are obtained for artificial mixture of oligomers and other forms of BChl *c* in model systems PVA. For the decay of fluorescence observed in a region of oligomeric emission (at 750 nm) it is enough to suppose only one monoexponential component, giving at various excitation wavelengths slightly different τ values at about 0.2 ns (Table I). From polarization absorption spectra (Fig. 3) there must be at least two oligomeric forms, but they have to have similar lifetimes. Global analysis give the value of this decay equal to 0.183 ns, but the accuracy of fitting is rather low. Previously [7] the largest decay component of this emission was found to have a lifetime from 0.001 ns till 0.01 ns for various light polarization. Now a strong component with short decay time is observed before global analysis at 680 nm observation, but after analysis the strong component with τ = 0.136 ns together with a much weaker component with a longer lifetime (about 4 ns) are observed (Table I). The light polarization does not critically change the contributions from the various decay components for unstretched film. It is interesting that now in both regions of observation the strongest component has a short lifetime from 0.136 ns to 0.183 ns whereas previously [7] for 670 nm observation slow component characteristic of monomer emission was also seen. The intensity of emission from monomers and small aggregates is comparable with the emission from oligomers (Fig. 4). The longer lifetime component is of course more easily seen in steady state emission spectra, but f_i are low for 680 nm observation. This suggests strong excitation energy transfer from monomers to oligomers responsible for shortening monomeric lifetimes. One should remember that even global analysis is to some degree an arbitrary mathematical procedure, very useful but not univocal and that oligomeric emission decay can be only in crude approximation be treated as uniexponential [10].

Lifetime Measurements of Bacteria and Bacteria Fragments in PVA

In data for 750 nm emission (Table II), shown without global analysis, the shortest component (from 0.002 ns to 0.238 ns), is strongest (highest amplitude). It is unexpected that shortest lifetimes are observed at 420 nm excitation in bacteria fragments. It seems that degradation products due to sonication are present. Analysis on three

Table I. Fluorescence Lifetime (Experimental and Global Analysis Data) for Mixtures of Oligomers and Other Forms of BChl *c* in PVA

		Experimental data					Global analysis				
λ_{exc} (nm)	λ_{em} (nm)	τ_i (ns)	α_i	f_i	$\langle\tau_i\rangle$ (ns)	χ^2	τ_i (ns)	α_i	f_i	$\langle\tau_i\rangle$ (ns)	χ^2
420	680	2.969	0.005	0.135	0.488	7.03	3.987	0.004	0.106	0.545	26.4
420	680	0.101	0.995	0.865	0.488	7.03	0.136	0.996	0.894	0.545	26.4
438	680	4.394	0.002	0.051	0.378	7.76	3.987	0.002	0.068	0.397	26.4
438	680	0.163	0.998	0.949	0.378	7.76	0.136	0.998	0.932	0.397	26.4
450	680	0.256	0.061	0.567	0.151	14.0	3.987	0.001	0.018	0.204	26.4
450	680	0.013	0.939	0.433	0.151	14.0	0.136	0.999	0.982	0.204	26.4
420	750	0.216	1.000	1.000	0.216	16.6	0.183	1.000	1.000	0.183	27.0
438	750	0.176	1.000	1.000	0.176	10.8	0.183	1.000	1.000	0.183	27.0
450	750	0.163	1.000	1.000	0.163	17.7	0.183	1.000	1.000	0.183	27.0

Table II. Fluorescence Lifetime (Experimental and Global Analysis Data) for Whole Bacteria Cells and Bacteria Fragments Embedded in PVA (λ_{em} = 750 nm)

		Experimental data					Global analysis				
Type of sample	λ_{exc} (nm)	τ_i (ns)	α_i	f_i	$\langle\tau_i\rangle$ (ns)	χ^2	τ_i (ns)	α_i	f_i	$\langle\tau_i\rangle$ (ns)	χ^2
Whole cells	420	6.160	0.193	0.807	5.161	3.56	6.131	0.191	0.802	5.128	8.08
	420	1.888	0.068	0.087	5.161	3.56	2.073	0.065	0.092	5.128	8.08
	420	0.209	0.739	0.106	5.161	3.56	0.208	0.744	0.106	5.128	8.08
	438	5.901	0.168	0.806	4.922	6.81	6.131	0.188	0.756	4.961	8.08
	438	1.312	0.111	0.118	4.922	6.81	2.073	0.109	0.148	4.961	8.08
	438	0.129	0.721	0.076	4.922	6.81	0.208	0.703	0.096	4.961	8.08
	450	5.134	0.087	0.793	4.214	10.7	6.131	0.145	0.630	4.444	8.08
	450	0.920	0.094	0.152	4.214	10.7	2.073	0.184	0.271	4.444	8.08
	450	0.038	0.819	0.055	4.214	10.7	0.208	0.671	0.099	4.444	8.08
Fragments	420	7.422	0.003	0.850	6.491	14.1	6.820	0.063	0.899	6.181	15.3
	420	2.036	0.001	0.088	6.491	14.1	1.251	0.014	0.037	6.181	15.3
	420	0.002	0.996	0.062	6.491	14.1	0.033	0.923	0.064	6.181	15.3
	438	6.763	0.166	0.883	6.080	6.98	6.820	0.102	0.883	6.126	15.3
	438	1.317	0.076	0.079	6.080	6.98	1.251	0.051	0.081	6.126	15.3
	438	0.064	0.758	0.038	6.080	6.98	0.033	0.847	0.036	6.126	15.3
	450	6.668	0.244	0.817	5.622	9.57	6.820	0.077	0.822	5.776	15.3
	450	1.869	0.112	0.106	5.622	9.57	1.251	0.067	0.133	5.776	15.3
	450	0.238	0.644	0.077	5.622	9.57	0.033	0.856	0.045	5.776	15.3

components give low χ^2. The τ_i from monomeric forms with 5 ns–7.5 ns lifetimes are rather high even by low amplitude, because of slow decay of such forms. From the same reason average $\langle\tau\rangle$ is rather high (4.2 ns–6.5 ns). Global analysis of whole bacteria and bacteria fragments (Table II) at 750 nm observation give different results for whole bacteria and for fragments. In fragments shortest lifetime (Table II) is about 0.03 ns whereas in whole bacteria it is about 0.21 ns. In both samples this is the main component of decay at 750 nm observation. At 680 nm observation (Table III) global analysis gives a much weaker short lifetime component and a stronger longest one (in fragments it is even about 9.5 ns in whole bacteria 6,1 ns). Previously[7], a long lifetime component, characteristic of monomeric emission was obtained at both regions of observation (670 nm and 750 nm) in bacteria and bacteria fragments. A short lifetime component at 750 nm observation was seen previously [7] at mutually perpendicular polarization of exciting and fluorescence beams in a sample with whole bacteria.

DISCUSSION

The polarized absorption and fluorescence spectra in various degrees of aggregation of BChl *c* in PVA

films show that several spectral properties of this pigment located in antenna of green bacteria can be reproduced on the basis of simple models. As previously reported [7,9,24] the absorption and fluorescence maxima of artificial oligomers and BChl *c* in chlorosomes are located in similar spectral regions as well as oligomers exhibit in both cases much higher degree of orientation than disaggregated BChl *c* and BPhe *c* [27]. From reversible aggregation and disaggregation of BChl *c* in chlorosomes [37] it is known that disaggregated BChl *c* is not removed from chlorosomes and that it has some different spectral properties than monomers of this pigment in solution [38]. The investigations *in vivo* of disaggregated forms of pigments with 670 nm absorption is complicated, because this region includes superimposed contributions from BChl *c*, BPhe *c* and some isomers of pigments that are not very well identified [12,15,26]. Such absorption increases as a result of chlorosome degradation. In our experiments this is due to cell fragmentation by sonication as well as a result of storage of PVA samples with bacteria or bacteria fragments [7,11,24,29]. The pigments are highly separated from the chain of the excitation energy transfer to reaction centers, because they exhibit effective photopotential generation [29] and fluorescence emission [24] and these processes are competing with excitation energy transfer to the reaction centers. In the present paper we focus our attention on the disaggregated pigments investigating the samples with high 670 nm absorption obtained by long storage of bacteria or bacteria fragments in PVA films and on comparison of their properties with properties of model systems containing both: disaggregated pigments and oligomers. It is possible that in living organisms partial disaggregation of chlorosomal BChl *c* can occur under some condition. It seems probable, because it is known that more than one type of oligomers is present in organisms and that some oligomers can be disrupted into small aggregates (probably tetramers) which absorb also in 670 nm region [26].

Such pigments, even at low concentration, can strongly change the transfer of excitation to the reaction center because energy transferred to it can be trapped and changed into heat or to fluorescence and therefore can not be used for photochemical reaction of photosynthesis [24,29]. It was shown [27] that BPhe *c* is able to transfer excitation energy to reaction centre. Therefore these disagregated pigments can play various role in organisms.

Polarized absorption spectra (Fig. 5) show that pigments absorbing at 670 nm region are in some extent oriented in organisms, whereas BChlc *c* molecules embedded in the same PVA matrix are practically randomly distributed (Fig. 3). Fluorescence emission in such model is practically unpolarized (Fig. 4; VVV/VVH $\cong$ 1), whereas in organisms VVV/VVH $>$ 1, meaning that emission is polarized. This effect is observed only for pigment molecules with Q_y transitions forming small angles with the stretching axis, others exhibit practically unpolarized fluorescence (VHV/VHH $\cong$ 1). It shows once more that the pool of molecules absorbing in 670 nm region, with emission in 670 nm–680 nm region is not uniform. Emission in a fluorescence region of oligomers is usually low in organisms, because of efficient excitation energy transfer to other pigments, but it is much stronger in a model system in which oligomers are final acceptors of excitation [24]. The yield of fluorescence of oligomers depend on their structures [39]; it can even be as high as 0.5. In a mixture of various forms of oligomers it can have various values. In bacteria and bacteria fragments thermal deactivation in 670 nm and 750 nm regions is comparable [24]. Thermal deactivation and excitation energy transfer are competitive processes. It can suggest comparable yields of fluorescence if both specious are separated from the donor-acceptor chain. In models, where monomer-oligomer excitation transfer probably exists the yields of both forms seems to be similar (comparison of Fig. 3 and Fig. 4). From the shape of the Soret band it follows that all samples are in some extend pheophytinized, but this process is most probable for bacteria fragments (Fig. 5b) and is low for model samples (Fig. 3). It seems that pheophytinization has a low influence on degree of orientation. Therefore it is not possible to distinguish BChl *c* from BPhe *c* on the basis of polarized spectra.

The lifetimes in the present paper are measured by method of frequency domains only for unstretched samples using completely unpolarized light. If a sample contains only three groups of chromophors, the analysis for both region of fluorescence observation will be characterized by the same sets of lifetimes values. For model system after global analysis (Table I) in both observation regions, a short lifetime components with τ about 0.14 ns (at 680 nm) or 0.18 ns (at 750 nm) predominates. Short lifetime components obtained from global analysis are longer than those usually observed for artificial oligomers [7,18,40,41]. Previously [7] short lifetime components about 0.06 ns–0.07 ns was observed for model systems of highly oligomerized samples. It seems that in the present model, excitation energy transfer from almost randomly distributed monomers to also non-ordered oligomers is very efficient and therefore a long lifetime component of monomeric pigment (6 ns–7 ns) is not observed even at 680 nm observation. From global analysis it seems that one specious is predominantly responsible for fluorescence emission, but this is not in agreement with fluorescence spectra in which monomers and oligo-

Table III. Fluorescence Lifetime (Experimental and Global Analysis Data) for Whole Bacteria Cells and Bacteria Fragments Embedded in PVA (λ_{em} = 680 nm)

		Experimental data					Global analysis				
Type of sample	λ_{em} (nm)	τ_i (ns)	α_i	f_i	$\langle\tau_i\rangle$ (ns)	χ^2	τ_i (ns)	α_i	f_i	$\langle\tau_i\rangle$ (ns)	χ^2
Whole cells	420	6.332	0.416	0.883	5.684	9.03	6.061	0.379	0.881	5.448	15.3
	420	0.845	0.390	0.110	5.684	9.03	1.008	0.270	0.104	5.448	15.3
	420	0.106	0.194	0.007	5.684	9.03	0.109	0.351	0.015	5.448	15.3
	438	6.300	0.309	0.858	5.610	11.1	6.061	0.343	0.908	5.573	15.3
	438	1.823	0.136	0.110	5.610	11.1	1.008	0.156	0.068	5.573	15.3
	438	0.132	0.555	0.032	5.610	11.1	0.109	0.501	0.024	5.573	15.3
	450	5.798	0.159	0.868	5.140	5.73	6.061	0.258	0.863	5.340	15.3
	450	1.049	0.100	0.099	5.140	5.73	1.008	0.185	0.103	5.340	15.3
	450	0.047	0.741	0.033	5.140	5.73	0.109	0.557	0.034	5.340	15.3
Fragments	420	7.659	0.347	0.916	7.093	13.1	9.449	0.236	0.535	7.226	23.7
	420	1.016	0.221	0.077	7.093	13.1	5.018	0.357	0.430	7.226	23.7
	420	0.046	0.432	0.007	7.093	13.1	0.358	0.404	0.035	7.226	23.7
	438	7.644	0.334	0.720	6.572	11.2	9.449	0.179	0.472	6.887	23.7
	438	4.557	0.179	0.230	6.572	11.2	5.018	0.342	0.480	6.887	23.7
	438	0.362	0.487	0.050	6.572	11.2	0.358	0.479	0.048	6.887	23.7
	450	6.428	0.275	0.881	5.785	7.2	9.449	0.093	0.307	6.057	23.7
	450	1.444	0.112	0.081	5.785	7.2	5.018	0.357	0.625	6.057	23.7
	450	0.125	0.613	0.038	5.785	7.2	0.358	0.550	0.068	6.057	23.7

mers clearly take part in emission. In steady state measurements longer lived species make larger contributions, but in lifetime measurement at 450 nm excitation and 680 nm observation f_1 of the longer component is higher than that of the shorter.

In the case of bacteria and bacteria fragments three different lifetime components have to be used. They are different for whole bacteria and for fragments and for observations at 680 nm and 750 nm (Tables II and III). It clearly shows that such an approach is an oversimplification and that global analysis in this approximation is not giving reasonable results. It means that pigments located in organism give slightly different lifetimes for every one type of pigment because of its different surrounding.

ACKNOWLEDGMENTS

Z. Gryczyński, I. Gryczyński, and B. Zelent were supported by NIH, National Center for Research resources (RR-08119). D. Frąckowiak, J. Goc, and A. Dudkowiak were supported by Polish KBN Grant 6 PO4A 010 17.

REFERENCES

1. J. H. Eggers and E. W. Thulstrup (1965) Zur Auswertung des Dichroismus von Elektronenspectren von in Folien Oroentirten Moleculen (Jablonski Methode), Lecture at 8th European Congress on Molecular Spectroscopy, Copenhagen.
2. J. Michl and E. W. Thulstrup (1986) *Spectroscopy with Polarized Light*, VCH, New York.
3. J. Breton and A. Vermeglio (1982) in Govindjee (Ed), *Photosynthesis*, Academic Press, New York, Vol. 1, pp. 153–193.
4. J. Miyake, T. Kusumi, A. Dudkowiak, J. Goc, and D. Frąckowiak (1998) *J. Photochem. Photobiol. A Chem.* **116**, 147–151.
5. A. Planner, J. Goc, A. Dudkowiak, D. Frąckowiak, and J. Miyake (1997) *J. Photochem. Photobiol. B Biol.* **39**, 73–80.
6. A. Jabłoński (1935) *Acta Phys. Polon.* **3**, 371–387.
7. D. Frąckowiak, A. Dudkowiak, A. Ptak, H. Malak, I. Gryczyński, and B. Zelent (1998) *J. Photochem. Photobiol. B Biol.* **44**, 231–239.
8. S. Surma and D. Frąckowiak (1970) *Photosynthetica* **4**, 202–213.
9. T. Martyński, D. Frąckowiak, J. Miyake, A. Dudkowiak, and A. Piechowiak (1998) *J. Photochem. Photobiol. B Biol.* **42**, 57–66.
10. A. Kowalczyk, H. Malak, B. Zelent, A. Dudkowiak, and D. Frąckowiak (1966) *Photosynthetica* **32**, 613–616.
11. A. Dudkowiak, R. Cegielski, A. Ptak, A. Planner, E. Chrzumnicka, I. Hanyż, and D. Frąckowiak (1994) *Photosynthetica* **30**, 183–191.
12. A. Dudkowiak, C. Francke, J. Amesz, A. Planner, I. Hanyż, and D. Frąckowiak (1996) *Spectrochim. Acta A* **52**, 251–264.
13. D. Frąckowiak (1978) *Acta Phys. Polon. A* **54**, 757–760.
14. D. Bauman and D. Wróbel (1980) *Biophys. Chem.* **12**, 83–91.
15. M. Fregata, B. Norden, and T. Kurucev (1988) *Photochem. Photobiol.* **47**, 133–143.
16. M. van Gurp, U. van Heide, J. Verhagen, T. Piters, G. van Gingel, and Y. K. Levine (1989) *Photochem. Photobiol.* **49**, 663–672.
17. V. H. Novoderozhkin and Z. G. Fetisova (1995) in P. Mathis (Ed.), *Photosynthesis: From Light to Biosphere*, Kluwer Academic, Dordrecht, Vol. I, pp. 99–102.
18. M. Mimuro, K. Matsuura, K. Shimada, Y. Nishimura, I. Yamazaki, M. Kobayashi, Z. Y. Wang, and T. Nozawa (1995) in P. Mathis (Ed.), *Photosynthesis: From Light to Biosphere*, Kluwer Academic, Dordrecht, Vol. 1, pp. 41–46.
19. J. M. Olson (1998) *Photochem. Photobiol.* **67**, 61–75.
20. R. E. Blankenship, J. M. Olson, and M. Miller (1995) in R. E. Blankenship, M. T. Madigan, and C. E. Bauer (Eds.), *Antenna*

Complexes from Green Photosynthetic Bacteria, Kluwer Academic, Dodrecht, pp. 399–435.
21. L. A. Staehelin, J. R. Golecki, R. C. Fuller, and G. Drews (1978) *Arch. Microbiol.* **119**, 269–277.
22. R. G. Feick and R. C. Fuller (1984) *Biochemistry* **23**, 3693–3700.
23. J. R. Lakowicz (1999) *Principles of Fluorescence Spectroscopy* 2nd ed., Kluwer Academic, Dodrecht.
24. A. Planner, B. Susta, M. Nowicki, K. Klaczyńska, and D. Frąckowiak (1999) *J. Fluores.* **9**, 139–143.
25. A. Dudkowiak, C. Francke, and J. Amesz (1995) *Photosynth. Res.* **46**, 427–433.
26. A. Dudkowiak, C. Francke, J. Amesz, A. Planner, and D. Frąckowiak (1996) *Spectrochim. Acta A* **52**, 1661–1669.
27. S. Tokita, M. Hirota, N.-U. Frigaard, K. Shimada, and K. Matsuura (1999) *Arch. Microbiol.* **172**, 40–44.
28. T. Swarthoff, H. J. M. Kramer, and J. Amesz (1982) *Biochim. Biophys. Acta* **681**, 354–358
29. A. Ptak, A. Dudkowiak, and D. Frąckowiak (1998) *J. Photochem. Photobiol. A Chem.* **115**, 63–68.
30. Z. Gryczyński, R. Paolesse, K. M. Smith, and E. Bucci (1997) *Biophys. Chem.* **69**, 71–84.
31. Z. Gryczyński, E. Bucci, and J. Kośba (1993) *Photochem. Photobiol.* **58**, 492–498.
32. S. C. M. Otte, J. C. van der Heiden, N. Pfenning, and J. Amesz (1991) *Photosynth. Res.* **28**, 78–87.
33. T. Ishii, K. Uehara, Y. Ozaki, and M. Mimuro (1999) *Photochem. Photobiol.* **70**, 760–765.
34. D. Frąckowiak, S. Hotchandani, and R. M. Leblanc (1983) *Photobiochem. Photobiophys.* **6**, 339–350.
35. A. N. Melkozernov, J. M. Olson, Y.-F. Li, J. P. Allen, and R. E. Blankenship (1998) *Photosynth. Res.* **56**, 315–328.
36. M. Mimuro, M. Hirota, Y. Nishimura, T. Moriyama, I. Yamazaki, K. Shimada, and K. Matsuura (1994) *Photosynth. Res.* **41**, 181–191.
37. K. Matsuura and J. M. Olson (1990) *Biochim. Biophys. Acta* **1019**, 233–238.
38. Y. Zhu, S. Lin, B. L. Ramakrishna, P. I. van Noort, and R. E. Blankenship (1996) *Photosynth. Res.* **47**, 207–218.
39. R. G. Alden, S. H. Lin, and R. E. Blankenship (1992) *J. Luminesc.* **51**, 51–66.
40. D. C. Brune, T. Nozawa, and R. E. Blankenship (1987) *Biochemistry* **26**, 8644–8652.
41. P. I. van Noort, Y. Zhu, R. LoBrutto, and R. E. Blankenship (1997) *Biophys. J.* **72**, 316–325.